



14 **ABSTRACT**

15           Gibberellin (GA) phytohormones are ubiquitous regulators of growth and developmental processes  
16 in vascular plants. The convergent evolution of GA production by plant-associated bacteria, including both  
17 symbiotic, nitrogen-fixing rhizobia and phytopathogens, suggests that manipulation of GA signaling is a  
18 powerful mechanism for microbes to gain an advantage in these interactions. Although homologous  
19 operons encode GA biosynthetic enzymes in both rhizobia and phytopathogens, notable genetic  
20 heterogeneity and scattered operon distribution in these lineages suggests distinct functions for GA in varied  
21 plant-microbe interactions. Therefore, deciphering GA operon evolutionary history could provide crucial  
22 evidence for understanding the distinct biological roles for bacterial GA production. To further establish  
23 the genetic composition of the GA operon, two operon-associated genes that exhibit limited distribution  
24 among rhizobia were biochemically characterized, verifying their roles in GA biosynthesis. Additionally,  
25 a maximum-parsimony ancestral gene block reconstruction algorithm was employed to characterize loss,  
26 gain, and horizontal gene transfer (HGT) of GA operon genes within alphaproteobacteria rhizobia, which  
27 exhibit the most heterogeneity among GA operon-containing bacteria. Collectively, this evolutionary  
28 analysis reveals a complex history for HGT of both individual genes and the entire GA operon, and  
29 ultimately provides a basis for linking genetic content to bacterial GA functions in diverse plant-microbe  
30 interactions.

31

## 32 INTRODUCTION

33 The clustering of bacterial biosynthetic genes within operons allows for the controlled co-  
34 expression of functionally-related genes under a single promoter, and the opportunity for these genes to be  
35 mobilized and co-inherited as a complete metabolic unit via horizontal gene transfer (HGT) [1, 2]. Because  
36 operons are responsible for many fundamental biosynthetic pathways in bacteria, analysis of the genetic  
37 structure of complex operons can provide important clues regarding the selective pressures driving the  
38 evolution of bacterial metabolism, and can also give insight into the occurrences and mechanisms of HGT.

39 The ability for bacteria to produce gibberellin (GA), a ubiquitous plant hormone, is imparted by a  
40 GA biosynthetic operon (GA operon; **Figure 1**), which is found in both nitrogen-fixing rhizobia and  
41 phytopathogenic bacteria [3–5]. While the diterpenoid GA phytohormones act as endogenous signaling  
42 molecules for growth and development in vascular plants [6], plant-associated fungi and bacteria have  
43 convergently evolved the ability to produce GA as a mechanism for host manipulation [4, 7–9]. The  
44 phenomenon of GA production by plant-associated microbes has important biological implications, as  
45 perturbation in GA signaling can lead to extreme phenotypic changes in plants. For example, production of  
46 GA by the rice pathogen *Gibberella fujikuroi* leads to dramatic elongation and eventual lodging of rice  
47 crops [10], and impaired GA metabolism is responsible for the semi-dwarf crop phenotypes associated with  
48 crops utilized within the Green Revolution [11, 12]. More recently, it has been shown that GA acts as a  
49 virulence factor for phytopathogenic bacteria [9], and can affect nodulation phenotypes when produced by  
50 rhizobia in symbiosis with legumes [4]. Therefore, studying the biosynthesis and biological function of  
51 microbial GA is crucial to our understanding of how these plant-microbe interactions can affect plant health  
52 and development.

53 The GA operon was discovered in the rhizobial symbiont of soybean, *Bradyrhizobium*  
54 *diazoefficiens* USDA 110 [13]. This operon contains a geranylgeranyl diphosphate synthase (*ggps*), two  
55 diterpene synthases/cyclases (*cps* and *ks*), three cytochrome P450 (CYP) monooxygenases (*cyp112*,  
56 *cyp114*, and *cyp117*), a short-chain dehydrogenase/reductase (*sdr<sub>GA</sub>*), and a ferredoxin (*fd<sub>GA</sub>*) [13, 14]. The

57 *B. diazoefficiens* operon also contains a severely truncated, presumably non-functional CYP gene (pseudo  
58 *cyp115*, or *p-cyp115*) located at the 5' end of the operon. The core gene cluster, which contains all of the  
59 aforementioned genes other than *cyp115*, is widely distributed in symbiotic nitrogen-fixing rhizobia from  
60 the alphaproteobacteria class ( $\alpha$ -rhizobia) [15], and biochemical characterization of GA operon genes in  
61 several  $\alpha$ -rhizobia, including *B. diazoefficiens*, *Sinorhizobium fredii*, and *Mesorhizobium loti*, has  
62 demonstrated that this core operon is responsible for biosynthesis of GA<sub>9</sub>, the penultimate intermediate to  
63 the bioactive phytohormone GA<sub>4</sub> [3, 4, 16–18]. While exclusively found in plant-associated bacteria [19],  
64 the GA operon exhibits scattered distribution within the  $\alpha$ -rhizobia, and functional versions of the operon  
65 can also be found in several betaproteobacterial rhizobia symbionts ( $\beta$ -rhizobia) [20, 21]. Analogous GA  
66 operons can be found in certain gammaproteobacterial plant pathogens as well (e.g. *Xanthomonas* and  
67 *Erwinia* species), and characterization of the GA operon from several distant gammaproteobacterial  
68 lineages has demonstrated that the biosynthetic functionality of this operon is conserved [5, 9, 20].

69 The abundance of sequenced bacterial genomes indicates that the GA operon structure is more  
70 complex and variable than that initially described for the  $\alpha$ -rhizobia *B. diazoefficiens* in which this operon  
71 was initially identified [14, 15]. Specifically, certain bacteria with the GA operon were found to contain a  
72 full length *cyp115* gene at the 5' end of the gene cluster, as opposed to a pseudo-gene/fragment, and this  
73 enzyme has been shown to catalyze the final step in bioactive GA biosynthesis, converting GA<sub>9</sub> into  
74 bioactive GA<sub>4</sub> [5, 20, 22]. Additionally, many bacterial strains possess a putative isopentenyl diphosphate  
75  $\delta$ -isomerase (*idi*) gene located at the 3' end of the operon, which presumably functions in balancing the  
76 concentrations of the (di)terpenoid building blocks, isopentenyl diphosphate (IPP) and dimethylallyl  
77 diphosphate (DMAPP) [23]. Full-length *cyp115* and *idi* genes are notably absent from many  $\alpha$ - and  $\beta$ -  
78 rhizobia with the operon, while copies of these genes are essentially always present in the GA operons of  
79 gammaproteobacterial phytopathogens (**Figure 1**). Intriguingly, it appears that some of the  $\alpha$ -rhizobia have  
80 specifically lost these genes, as fragments of both *cyp115* and *idi* can be found flanking the core gene cluster  
81 in many of the relevant species/strains [22, 24]. Moreover, a small number of  $\alpha$ -rhizobia have a presumably

82 inactivating frameshift mutation in the canonical *ggps* within their operon, but have an additional isoprenyl  
83 diphosphate synthase (IDS) gene adjacent to the operon (*ids2*) [17], which could potentially compensate  
84 for the loss of *ggps*. Overall, this heterogeneity of the GA operon in rhizobia provides an excellent  
85 opportunity for analyzing the formation and reorganization of bacterial gene clusters.

86 Initial phylogenetic analyses of the GA operon suggested that it may have undergone HGT among  
87 bacterial lineages [17, 20]. Furthermore, the varying genetic structure of the operon in divergent species,  
88 including both symbionts and pathogens, suggests that selective pressures unique to certain bacteria may  
89 be driving the acquisition or loss of not only the GA operon, but also some of the associated genes. Thus,  
90 detailed analysis of GA operon evolution will help elucidate the evolutionary processes that have shaped  
91 bacterial GA biosynthesis in plant-microbe interactions. Here, the predicted biochemical functions were  
92 assessed and confirmed for the *idi* and *ids2* genes that are sporadically associated with the GA operon,  
93 thereby providing evidence for their roles in GA biosynthesis. This clarification of genetic content prompted  
94 further analysis of the distribution and function of the GA operon in bacteria more generally, thereby  
95 providing an overview of the genetic diversity and evolutionary history of this gene cluster. Using an  
96 algorithm developed to analyze the assembly and evolution of gene blocks (i.e. genes within  
97 operons/clusters) [25], the distribution and phylogeny of the GA operon was further analyzed within the  $\alpha$ -  
98 rhizobia, which display a large amount of diversity in operon structure and genetic content. Altogether, this  
99 thorough assessment of the underlying genetics and biochemistry of the GA operon allows for the  
100 formulation of informed hypotheses regarding the biological function of GA production within diverse  
101 bacterial lineages.

102

103

## 104 RESULTS

### 105 Biochemical characterization of two accessory GA operon genes

106 Given that most bacteria do not normally produce (*E,E,E*)-geranylgeranyl diphosphate (GGPP), a  
107 necessary precursor, GA biosynthesis requires the presence of a *ggps* gene. In the GA operon-containing  
108 strain *Rhizobium etli* CFN 42, the operon *ggps* contains a frameshift mutation that results in a severely  
109 truncated protein [17]. However, a second predicted IDS gene (*ids2*), albeit with low sequence identity to  
110 the canonical operon *ggps* found in other *Rhizobium* species (<30% at the amino acid level), is found in  
111 close proximity to this strain's operon (**Figure 1**), as well as in several other  $\alpha$ -rhizobia in which *ggps*  
112 similarly appears to be inactive. Given the conservation of these modified operons, we hypothesized that  
113 the encoded IDS2 also produces GGPP, thereby restoring functionality to these GA operons. Indeed,  
114 recombinantly expressed IDS2 from *R. etli* CFN42 (*ReIDS2*) produced GGPP as its sole product from the  
115 universal isoprenoid precursors IPP and DMAPP (**Supplementary Figure 1**). Thus, IDS2 can functionally  
116 complement the loss of the canonical *ggps* to restore production of GA in these operons. Accordingly,  
117 hereafter these *ids2* gene orthologs are referred to as *ggps2* to reflect their biochemical function (e.g.  
118 *ReIDS2* becomes *ReGGPS2*).

119 The only remaining gene strongly associated with the GA operon but not yet characterized was *idi*,  
120 which has been presumed to be involved in balancing the ratio of IPP and DMAPP isoprenoid building  
121 blocks for diterpenoid biosynthesis [23]. The GA operon *idi* from *Erwinia tracheiphila* (*EtIDI*), a  
122 gammaproteobacteria plant pathogen, was cloned and heterologously expressed in *E. coli*. To test for  
123 activity, a coupled enzyme assay with *EtIDI* and *ReGGPS2* was employed. Because IDS enzymes require  
124 both IPP and DMAPP as substrates, *ReGGPS2* is unable to produce GGPP with only IPP or DMAPP alone  
125 as substrate. Addition of *EtIDI* into these reactions enabled the production of GGPP by *ReGGPS2* from  
126 either IPP or DMAPP alone (**Supplementary Figure 2**), thus indicating that *EtIDI* can effectively  
127 interconvert these.

128

## 129 HGT of the GA operon within alphaproteobacterial rhizobia

130 The scattered distribution of the GA operon among three classes of proteobacteria suggests HGT  
131 of this gene cluster. Previous phylogenetic analysis suggests that the ancestral gene cluster initially evolved  
132 within gammaproteobacterial phytopathogens, as their operon genes exhibit greater phylogenetic  
133 divergence than those in the rhizobia, and that the operon was subsequently acquired by  $\alpha$ - and  $\beta$ - rhizobia  
134 in separate HGT events [20]. Additionally, specific phylogenetic analysis of the GA operon within  $\alpha$ -  
135 rhizobia suggests that it may have subsequently undergone additional HGT within this class [17].

136 It has previously been noted that the GC content of the GA operon in rhizobia is particularly high  
137 compared with the surrounding genomic sequence [14, 24, 26, 27], a phenomenon that is often associated  
138 with HGT [28]. To better assess the increased GC content of the GA operon, we analyzed the gene cluster  
139 sequences and the surrounding DNA in exemplaries from four of the major  $\alpha$ -rhizobia genera  
140 (*Bradyrhizobium*, *Mesorhizobium*, *Rhizobium*, and *Sinorhizobium*) and two genera of the  
141 gammaproteobacterial plant pathogens (*Erwinia* and *Xanthomonas*). In each case, the GA operon has  
142 noticeably higher GC content than the surrounding DNA (>10% higher), with sharp drops in GC content  
143 preceding and following the operon (**Supplementary Figure 3**). Further support for HGT of the GA operon  
144 has been suggested by the presence of insertional sequence (IS) elements flanking the operon (e.g.  
145 transposases and integrases) in many species [5, 22]. Overall, these collective observations strongly support  
146 HGT of the GA operon, consistent with its widely-scattered distribution throughout the proteobacteria.

147 As an added layer of complexity, it is generally accepted that the large symbiotic or pathogenic  
148 genomic islands or plasmids (i.e. symbiotic or pathogenic modules), which are associated with the plant-  
149 associated lifestyle of the bacteria in question, are capable of undergoing HGT [29]. For  $\alpha$ -rhizobia strains  
150 where sufficient genomic information is available, the GA operon is invariably found within the symbiotic  
151 module [24, 26, 27, 30–32]. Thus, there may be multiple levels of HGT with the GA operon in  $\alpha$ -rhizobia:

152 one in which the entire symbiotic module, including a GA operon, is transferred, and one in which the GA  
153 operon alone is transferred. Indeed, this double-layered HGT for the GA operon has been previously  
154 suggested based on phylogenetic incongruences between genes representative of species (16S rRNA),  
155 symbiotic modules (*nifK*), and GA operon (*cps*) similarity [17].

156

### 157 **Gene cluster analysis**

158 While the GA operons found in gammaproteobacteria exhibit essentially uniform gene content and  
159 structural composition, those from the  $\alpha$ -rhizobia exhibit much more diversity in genetic structure. This  
160 suggests that selective pressures specific to the rhizobia, presumably their symbiotic relationship with  
161 legumes, may have driven this heterogeneity in the operon. To better understand the evolutionary history  
162 of the GA operon in the  $\alpha$ -rhizobia, a more thorough analysis was carried out with Reconstruction of  
163 Ancestral Genomes Using Events (ROAGUE) software [25, 33]. ROAGUE generates a phylogenetic tree  
164 with selected taxa that contain gene blocks (i.e. gene clusters) of interest, and then uses a maximum  
165 parsimony approach to reconstruct a predicted gene block structure at each ancestral node of the tree. Using  
166 the ROAGUE method, the evolutionary events involved in the genetic construction of orthologous GA  
167 operon gene blocks in the  $\alpha$ -rhizobia, specifically gene loss, gain, and duplication, were quantitatively  
168 assessed (see **Supplementary Figure 4** for a summary of the method pipeline). A total of 118  $\alpha$ -rhizobia  
169 with the GA operon were included in this analysis. The most phylogenetically distant GA operon to those  
170 in the  $\alpha$ -rhizobia is found within *E. tracheiphila*, and as such this was used as an outgroup. Additionally, to  
171 observe the relative relationship between alpha- and gamma- proteobacterial operons, the GA operon from  
172 *Xanthomonas oryzae* was also included in the analysis.

173 An initial reconstruction was made by creating a species tree using the amino acid sequence of  
174 *rpoB* (RNA polymerase  $\beta$  subunit) from each strain as the phylogenetic marker gene (“full species tree” or  
175 *FS*) (**Supplementary Figure 5**). However, the species tree is rarely indicative of a given gene’s evolution,



176 and even less so concerning operon evolution where HGT is involved. To better understand the evolution  
177 of the GA operon in relationship to the bacterial species, we constructed a second tree with concatenated  
178 protein sequences comprising the core GA operon (“full operon tree” or *FO*) (**Supplementary Figure 6**).  
179 Due to the large number of species being analyzed, along with apparent phylogenetic redundancy that could  
180 introduce bias, reconstructions were also made with only the more distinct representative strains by using  
181 the Phylogenetic Diversity Analyzer (PDA) program, which reduced the number of analyzed taxa to 64  
182 [34]. These reduced phylogenetic trees are referred to as the “partial species tree” or *PS* (**Figure 2**), and the  
183 “partial operon tree” or *PO* (**Figure 3**).

184 The ability of different ancestral reconstructions to capture the likely vertical evolution of a gene  
185 cluster can be assessed by the number of events (loss, gain, and duplication) calculated by this method, with  
186 a lower number of events indicating a more parsimonious reconstruction. From this analysis, it was found  
187 that fewer evolutionary events are reconstructed in *FO* (75 events) than in *FS* (121 events) (**Supplementary**  
188 **Figures 5 & 6**), with the same relative trend observed with the partial trees (62 events for *PO* vs. 78 events  
189 for *PS*) (**Figures 2 & 3**). The greater parsimony (i.e. fewer reconstructed events) observed in  
190 reconstructions built with alignments of the concatenated GA operon strongly supports the previously  
191 suggested hypothesis of HGT among  $\alpha$ -rhizobia [17]. Accordingly, the reconstructions based on GA operon  
192 similarity (i.e. *FO* and *PO*) were used for further analyses of operon inheritance.

193 In contrast to the phytopathogens, a full-length *cyp115* gene is absent from the genomes of most  
194 rhizobia (including both  $\alpha$ - and  $\beta$ - rhizobia), which typically have only the core operon and thus can only  
195 produce the penultimate intermediate GA<sub>9</sub> rather than bioactive GA<sub>4</sub> [18, 20, 22]. ROAGUE analysis  
196 indicates that *cyp115* loss occurred soon after  $\alpha$ -rhizobia acquisition of the GA operon, as the reconstructed  
197 ancestral node that connects the  $\alpha$ -rhizobia to *X. oryzae* (and the rest of the gammaproteobacteria) does not  
198 contain *cyp115* (**Figure 3**). Although the  $\alpha$ -rhizobia presumably acquired their GA operon from a  
199 gammaproteobacterial ancestor, the gammaproteobacteria seem to always have *cyp115* at the 5' end of the  
200 operon. In contrast, the  $\alpha$ -rhizobia typically only have a partial *cyp115* pseudo-gene/fragment located at

201 this position, as previously described [14, 22]. This suggests that the original operon acquired by an  $\alpha$ -  
202 rhizobia ancestor contained *cyp115*, and that this gene was subsequently lost.

203 Although most rhizobia have lost *cyp115*, a subset of  $\alpha$ -rhizobia (<20%) with the GA operon also  
204 have a full-length, functional *cyp115*. However, only in one strain (*Mesorhizobium* sp. AA22) does the GA  
205 operon have *cyp115* in the same location as in gammaproteobacterial GA operons [22]. Strikingly,  
206 ROAGUE analysis indicates that full-length *cyp115* has been regained independently in at least three  
207 different lineages, which is apparent in either the *PS* or *PO* reconstructions (**Figures 2 & 3**). Indeed, other  
208 than in *Mesorhizobium* sp. AA22, these full-length *cyp115* reside in alternative locations relative to the rest  
209 of the GA operon (e.g. 3' end of operon, or distally located), as previously described [22], which further  
210 supports independent acquisition via an additional HGT event.

211 Unlike *cyp115*, the *idi* gene seems to have been more widely retained by  $\alpha$ -rhizobia, as >50 of these  
212 strains possess this gene, which seems to invariably exhibit analogous positioning – i.e. as found in the  
213 gammaproteobacterial GA operons. This indicates loss of *idi* in many strains, albeit with notable differences  
214 among the major  $\alpha$ -rhizobia genera. For example, while the presence of *idi* appears to be almost random  
215 within *Rhizobium* (16/26 strains) and *Sinorhizobium/Ensifer* (8/14), it is nearly absent from all  
216 *Bradyrhizobium* (2/40), but ubiquitously found in *Mesorhizobium* (36/36).

217 Not surprisingly, *ggps2* seems to be invariably associated with operons in which the canonical *ggps*  
218 is inactive (**Figures 2 & 3**), and is only found in 13  $\alpha$ -rhizobia (of the 118 strains analyzed here). However,  
219 the ancestral reconstructions further indicate that *ggps2* is present in at least two distinct clades in all trees;  
220 one composed of closely related *Rhizobium* strains, and another with two *Bradyrhizobium* strains. While  
221 the *Rhizobium* all have homologous mutations in *ggps*, with similar positioning of *ggps2* (within 500 bp of  
222 the 3' end of the operon), the two *Bradyrhizobium* have distinct *ggps* mutations, with *ggps2* positioned on  
223 opposite sides of the operon. This suggests that, following initial acquisition of *ggps2*, this was further  
224 propagated via additional HGT events, in each case to complement inactivation of the canonical *ggps*, along

225 with subsequent vertical transmission at least in *Rhizobium*, similar to the observed re-acquisition of *cyp115*  
226 noted above.

227 In addition to ancestral gene loss and gain events, there further have been fusions between  
228 neighboring biosynthetic genes within the GA operon. In some  $\alpha$ -rhizobia, the *fd<sub>GA</sub>* gene, which is usually  
229 a distinct coding sequence, is found in-frame with either the 5' proximal *cyp114* gene, or the 3' proximal  
230 *sdr<sub>GA</sub>* gene, resulting in either *cyp114-fd* or *fd-sdr* fusions, which presumably encode bifunctional proteins.  
231 As fusion events are not analyzed by ROAGUE, these were assessed and categorized manually  
232 (**Supplementary Tables 1 & 2**). The *cyp114-fd* fusion is only found in a single clade consisting almost  
233 entirely of *Rhizobium* species, which is most evident in the *FO* reconstruction (**Supplementary Figure 6**).  
234 By contrast, while the *fd-sdr* fusion is largely found in a clade consisting of mostly *Mesorhizobium* species  
235 (**Supplementary Figure 6**), including *M. loti* MAFF303099 where activity of the fused Fd-SDR has been  
236 biochemically verified [4], such fusions appear to have independently occurred in other clades of  $\alpha$ -  
237 rhizobia. Beyond these multiple observations in  $\alpha$ -rhizobia, it should be noted that a *fd-sdr* fusion appears  
238 to have independently arisen in the  $\beta$ -rhizobia as well [21], further indicating that this is not functionally  
239 problematic.

240

## 241 **DISCUSSION**

242 Collectively, our analyses demonstrate a complex history of GA operon function, distribution, and  
243 evolution within the proteobacteria (**Figure 4**). Critical to this analysis was characterization of the *ggps2*  
244 and *idi* genes. Although these were previously noted to be associated with the GA operon, their function  
245 had not yet been demonstrated. To our knowledge, the *ggps2* and *idi* genes were the only remaining  
246 uncharacterized genes associated with the GA operon, and thus characterizing the enzymes encoded by  
247 these genes represents the final step in elucidation of the associated biosynthetic capacity. Given that  
248 bacteria typically produce both isoprenoid precursors IPP and DMAPP directly via the methyl-erythritol-

249 phosphate (MEP) pathway [23], an IDI is not strictly required, though it is possible that the presence of the  
250 *idi* gene would allow for increased flux towards GA by balancing precursor supply. Since the *idi* gene is  
251 ubiquitous in phytopathogen GA operons and has been lost multiple times in rhizobia, it may be that this  
252 gene optimizes GA production, which presumably assists use of GA as a virulence factor by the  
253 phytopathogens. However, the utility of optimized GA production by rhizobia is not evident, and thus it is  
254 not clear why some  $\alpha$ -rhizobia lineages retain this gene.

255         Unlike the isoprenoid precursor molecules, GGPP is not normally produced by most bacteria, and  
256 thus verification of *ggps2* as a GGPP synthase clarifies that GA biosynthesis is still possible in rhizobia  
257 where the original operon *ggps* is no longer functional. Interestingly, the *ggps2*-containing *Rhizobium*  
258 lineage also harbors a previously defined mutation in the *cps* gene that has been shown to affect product  
259 outcome [35]. In particular, the otherwise conserved asparagine from the catalytic base dyad is replaced  
260 with a serine in this lineage, which results in predominant production of a distinct compound unrelated to  
261 GA biosynthesis (8 $\beta$ -hydroxy-*ent*-copalyl diphosphate), along with small amounts of the relevant GA  
262 intermediate (*ent*-copalyl diphosphate). Although retention of the operon indicates that the associated  
263 production of GA still provides a selective advantage to these *Rhizobium* strains, despite the presumably  
264 reduced flux, it is tempting to speculate that this observation reflects genetic drift of the *cps* in the interlude  
265 between loss of *ggps* and acquisition of *ggps2*.

266         The ROAGUE analysis reported here is consistent with the hypothesis that the GA operon has  
267 undergone HGT between various plant-associated bacteria, including phytopathogenic  
268 gammaproteobacteria and symbiotic, nitrogen-fixing  $\alpha$ - and  $\beta$ - rhizobia. Indeed, there appear to be three  
269 layers of HGT relevant to GA production that occur within the  $\alpha$ -rhizobia: 1) acquisition of the symbiotic  
270 module (i.e. symbiotic plasmid or genomic island), either with or without the GA operon, the latter of which  
271 can be followed by 2) separate acquisition of the GA operon within the symbiotic module, with the GA  
272 operon enabling 3) subsequent acquisition of auxiliary genes, including *ggps2* and, more interestingly,  
273 *cyp115*. Although widespread within proteobacteria, the GA operon has thus far only been found in plant-

274 associated species [19]. While this is not surprising due to the function of GA as a phytohormone, it  
275 emphasizes that such manipulation of host plants is an effective mechanism for bacteria to gain a selective  
276 advantage. Indeed, the ability to produce GA seems to be a powerful method of host manipulation for plant-  
277 associated microbes more generally, as certain phytopathogenic fungi also have convergently evolved the  
278 ability to produce GA as a virulence factor [8, 36].

279         Despite wide-ranging HGT of the GA operon between disparate classes of proteobacteria, its  
280 scattered distribution within each of these classes strongly indicates that the ability to produce GA only  
281 provides a selective advantage under certain conditions. This is evident for both symbiotic rhizobia and  
282 bacterial phytopathogens. For example, the GA operon is selectively found in the *oryzicola* pathovar of *X.*  
283 *oryzae*, where the resulting GA acts as a virulence factor suppressing the plant jasmonic acid (JA) induced  
284 defense response [9, 37, 38]. By contrast, production of GA by the  $\alpha$ -rhizobia *M. loti* MAFF303099 limits  
285 the formation of additional nodules, apparently without a negative impact on plant growth [4].

286         The occurrence of GA operon fragments (i.e. presence of some, but not all necessary biosynthetic  
287 operon genes) in many rhizobia indicates that production of GA is not advantageous in all rhizobia-legume  
288 symbioses. For example, at the onset of this study we identified >160  $\alpha$ -rhizobia with an obvious homolog  
289 of at least one GA operon gene, yet only ~120 of these contained a gene cluster (i.e. two or more  
290 biosynthetic genes clustered together), and ~20% of these clusters (26 of the 120  $\alpha$ -rhizobia operons  
291 analyzed here) are clearly non-functional due to the absence of key biosynthetic genes, consistent with  
292 dynamic selective pressure. It has been suggested that the GA operon is associated with species that inhabit  
293 determinate nodules [17], as these nodules grow via cell expansion (an activity commonly associated with  
294 GA signaling [39]), rather than indeterminate nodules, which grow via continuous cell division [40].  
295 However, while the presence of the GA operon does seem to be somewhat enriched within rhizobia that  
296 associate with determinate nodule-forming legumes, there are many examples of rhizobia with complete  
297 GA operons that were isolated from indeterminate nodules. For example, while most GA operon-containing  
298 *Bradyrhizobium* species associate with determinate nodule-forming plants, many species from the

299 *Ensifer/Sinorhizobium*, *Mesorhizobium*, and *Rhizobium* genera with the operon were isolated from  
300 indeterminate nodules, as were all three of the  $\beta$ -rhizobia with the GA operon (Integrated Microbe  
301 Genomes, JGI). This raises the question of why only some rhizobia have acquired and maintained the GA  
302 operon, and thus the capacity to produce GA.

303 In addition to its scattered distribution, the operon exhibits notable genetic diversity within the  $\alpha$ -  
304 rhizobia. For example, ROAGUE analysis indicates that loss of the usual *ggps* and subsequent recruitment  
305 of *ggps2* has been followed by HGT of this to other operons in which *ggps* has been inactivated, while *idi*  
306 appears to have independently lost several times. Similarly, fusion of *fd*<sub>GA</sub> with either the preceding *cyp114*  
307 or following *sdr*<sub>GA</sub> also appears to have occurred multiple times in  $\alpha$ -rhizobia, and certainly separately in  
308  $\beta$ -rhizobia [21]. Although loss of *idi* and such gene fusions may affect the rate of GA production, it appears  
309 that this can be accommodated in the symbiotic rhizobia-legume interaction. Indeed, the expression of the  
310 GA operon is delayed in this relationship [18], perhaps to mitigate any deleterious effects of GA during  
311 early nodule formation, which has been shown to be inhibitory to nodule formation, at least at higher  
312 concentrations [41].

313 Perhaps the most striking evolutionary aspect of the rhizobial GA operons is the early loss and  
314 scattered re-acquisition of *cyp115* in  $\alpha$ -rhizobia. While almost all  $\alpha$ -rhizobia GA operons contain only  
315 remnants of *cyp115* at the position in the GA operon where it is found in gammaproteobacteria  
316 phytopathogens [22], there is one strain (*Mesorhizobium* sp. AA22) where a full-length copy is found at  
317 this location. Phylogenetic analysis further suggests that this *cyp115* from *Mesorhizobium* sp. AA22 is  
318 closest to the ancestor of all the full-length copies found in  $\alpha$ -rhizobia, which are otherwise found at varied  
319 locations relative to the GA operon [22]. The ROAGUE analysis reported here indicates that *cyp115* was  
320 lost shortly after acquisition of the ancestral GA operon by  $\alpha$ -rhizobia, despite full-length copies being  
321 present in several different lineages. Accordingly, these results support the hypothesis that *cyp115* has been  
322 re-acquired by this subset of rhizobia via independent HGT events. Notably, while not recognized in the  
323 original report [4], this includes *M. loti* MAFF303099, the only strain in which the biological role of

324 rhizobial production of GA has been examined. Because *cyp115* is required for endogenous production of  
325 bioactive GA<sub>4</sub> from the penultimate (inactive) precursor GA<sub>9</sub>, this highlights the question of the selective  
326 pressures driving evolution of GA biosynthesis in rhizobia.

327         The contrast between GA operon-containing bacterial lineages provides a captivating rationale for  
328 the further scattered distribution of *cyp115* in rhizobia. In particular, the phytopathogens all contain *cyp115*  
329 and are thus capable of direct production of bioactive GA<sub>4</sub>, which serves to suppress the JA-induced plant  
330 defense response [9]. This observation naturally leads to the hypothesis that rhizobial production of GA<sub>4</sub>  
331 might negatively impact the ability of the host plant to defend against microbial pathogens invading the  
332 roots or root nodules, which would compromise the efficacy of this symbiotic interaction. Such detrimental  
333 effect of rhizobial production of bioactive GA<sub>4</sub> may have driven loss of *cyp115*. However, this would also  
334 result in a loss of GA signaling, as GA<sub>9</sub>, the product of an operon missing *cyp115*, presumably does not  
335 exert hormonal activity [42]. One possible mechanism to compensate for *cyp115* loss would be legume host  
336 expression of the functionally-equivalent plant GA 3-oxidase (GA3ox) gene (from endogenous plant GA  
337 metabolism) within the nodules in which the rhizobia reside. Expression of this plant gene would alleviate  
338 the necessity for rhizobial symbiont maintenance of *cyp115*, and would further allow the host to control the  
339 production of bioactive GA<sub>4</sub>, and thereby retain the ability mount an effective defense response when  
340 necessary. Re-acquisition of *cyp115* might then be driven by a lack of such GA3ox expression in nodules  
341 by certain legumes. However, this scenario remains hypothetical - though precisely controlled GA  
342 production by the plant has been shown to be critical for normal nodulation to occur [41, 43], coordinated  
343 biosynthesis of GA<sub>4</sub> by rhizobia and the legume host would need to be demonstrated. This includes both  
344 the transport of GA<sub>9</sub> from microbe to host plant, as well as subsequent conversion of this precursor to a  
345 bioactive GA (e.g. GA<sub>4</sub>). Accordingly, continued study of the GA operon will provide insight into the  
346 various roles played by bacterially-produced GA in both symbiotic rhizobia-legume relationships, as well  
347 as antagonistic plant-pathogen interactions, which in turn can be expected to provide fundamental  
348 knowledge regarding the ever-expanding roles of GA signaling in plants.



349

## 350 **METHODS**

### 351 **Biochemical characterization of *ReIDS2* and *EtIDI***

352 *ReIDS2* and *EtIDI* were cloned from *Rhizobium etli* CE3 (a streptomycin-resistant derivative of *R.*  
353 *etli* CFN42) [44] or *Erwinia tracheiphila* PSU-1, respectively, into pET101/D-TOPO (Invitrogen). The  
354 resulting 6xHis-tagged expression constructs were utilized to generate recombinant enzymes that were  
355 purified via Ni-NTA agarose (Qiagen). IDS enzyme assays were carried out in triplicate as previously  
356 described [45]. Detailed protocols for these experimental procedures can be found in the Supplemental  
357 Information document.

358

### 359 **Operon phylogenetic reconstruction**

#### 360 *Data acquisition*

361 Initial BLAST analysis (on April 12, 2017) revealed 166 bacterial strains that contain homologs of  
362 one or more of the GA operon genes. Given a set of 166 species/strain names, the corresponding genome  
363 assembly files were retrieved from the NCBI website. Using their assembly\_summary.txt file, the strains'  
364 genomic *fna* (fasta nucleic acid) files were downloaded. The number of strains analyzed was further reduced  
365 by only including strains with multiple GA operon genes (>2) clustered together, resulting in a final total  
366 of 118 strains. Retrieved genome assemblies for these strains were then annotated using Prokka [46].

#### 367 *Identifying orthologous gene blocks*

368 The terms reference taxa, neighboring genes, gene blocks, events, and orthologous gene blocks or  
369 orthoblocks have been described previously [25]. Briefly, the *reference taxon* is a strain in which the operon  
370 in question has been experimentally validated. Two genes are considered *neighboring genes* if they are 500  
371 nucleotides or fewer apart and on the same strand. A *gene block* comprises no fewer than two such



372 neighboring open reading frames. Organisms have *orthoblocks* when each has at least two neighboring  
373 genes that are homologous to genes in a gene block in the reference taxon's genome. Using *Xanthomonas*  
374 *oryzae* pv. *oryzicola* BLS256 (*Xoc*) as a reference taxon, we retrieved the 10 genes in the GA operon  
375 (*cyp115*, *cyp112*, *cyp114*, *fd<sub>GA</sub>*, *sdr<sub>GA</sub>*, *cyp117*, *ggps*, *cps*, *ks*, and *idi*). From those 10 genes, we determined  
376 whether a query strain contains orthologous gene blocks. An *event* is a change in the gene block between  
377 any two species with homologous gene blocks. We identify three types of pairwise events between  
378 orthoblocks in different taxa: splits, deletions, and duplications. The event-based distance between any two  
379 orthoblocks is the sum of the minimized count of splits, duplications, and deletions.

### 380 *Computational Reconstruction of the Gibberellin Operon Phylogeny*

381 ROAGUE (Reconstruction of Ancestral Gene blocks Using Events) software was used to  
382 reconstruct ancestral gene blocks. ROAGUE accepts as input (1) a set of extant bacterial genomes, (2) a  
383 phylogenetic tree describing the relatedness between the set of species, and (3) a gold standard operon that  
384 has been experimentally validated from one species in the set of given genomes. ROAGUE finds the  
385 orthologs of the genes in the reference operons, then constructs the hypothesized ancestral gene blocks  
386 using a maximum parsimony algorithm, as previously described [33]. To assess the possibility of HGT  
387 among rhizobia species, phylogenetic trees were constructed using both a species marker gene (*rpoB*) and  
388 a concatenation of the protein sequences for genes in the GA operon. The topology for each of these  
389 reconstructions was then compared in order to find major incongruences between the two that may indicate  
390 HGT. For details see Figure 2 and the Supplementary Materials.

391

### 392 **ACKNOWLEDGMENTS**

393 The authors thank Dr. Axel Schmidt and Prof. Jonathan Gershenzon (Max Planck Institute of  
394 Chemical Ecology) for use of their LC-MS/MS.

395

396 **FUNDING**

397 This work was supported by grants to RJP from the NIH (GM076324) and USDA (NIFA-AFRI grant 2014-  
398 67013-21720), a postdoctoral fellowship to RN from the Deutsche Forschungsgemeinschaft (DFG) NA  
399 1261/1-2, NSF ABI Development award 1458359 and NSF ABI Innovation award 1551363 to IF, a  
400 Discovery Grant and an Engage Grant, both from Natural Sciences and Engineering Research Council of  
401 Canada (NSERC) to TCC, and an Ontario Graduate Scholarship to AM.

402

403 **REFERENCES**

- 404 1. Fondi M, Emiliani G, Fani R. Origin and evolution of operons and metabolic pathways. *Res*  
405 *Microbiol* 2009; **160**: 502–512.
- 406 2. Lawrence JG, Roth JR. Selfish operons: Horizontal transfer may drive the evolution of gene  
407 clusters. *Genetics* 1996; **143**: 1843–1860.
- 408 3. Nett RS, Montanares M, Marcassa A, Lu X, Nagel R, Charles TC, et al. Elucidation of gibberellin  
409 biosynthesis in bacteria reveals convergent evolution. *Nat Chem Biol* 2017; **13**: 69–74.
- 410 4. Tatsukami Y, Ueda M. Rhizobial gibberellin negatively regulates host nodule number. *Sci Rep*  
411 2016; **6**: 27998.
- 412 5. Nagel R, Turrini PCG, Nett RS, Leach JE, Verdier V, Van Sluys MA, et al. An operon for  
413 production of bioactive gibberellin A4 phytohormone with wide distribution in the bacterial rice  
414 leaf streak pathogen *Xanthomonas oryzae* pv. *oryzicola*. *New Phytol* 2017; **214**: 1260–1266.
- 415 6. Hedden P, Thomas SG. Gibberellin biosynthesis and its regulation. *Biochem J* 2012; **444**: 11–25.
- 416 7. MacMillan J. Occurrence of gibberellins in vascular plants, fungi, and bacteria. *J Plant Growth*  
417 *Regul* 2002; **20**: 387–442.

- 418 8. Wiemann P, Sieber CMK, von Bargaen KW, Studt L, Niehaus EM, Espino JJ, et al. Deciphering  
419 the cryptic genome: Genome-wide analyses of the rice pathogen *Fusarium fujikuroi* reveal  
420 complex regulation of secondary metabolism and novel metabolites. *PLoS Pathog* 2013; **9**:  
421 e1003475.
- 422 9. Lu X, Hershey DM, Wang L, Bogdanove AJ, Peters RJ. An *ent*-kaurene-derived diterpenoid  
423 virulence factor from *Xanthomonas oryzae* pv. *oryzicola*. *New Phytol* 2015; **206**: 295–302.
- 424 10. Silverstone AL, Sun T ping. Gibberellins and the green revolution. *Trends Plant Sci* 2000; **5**: 1–2.
- 425 11. Peng J, Richards DE, Hartley NM, Murphy GP, Devos KM, Flintham JE, et al. ‘Green revolution’  
426 genes encode mutant gibberellin response modulators. *Nature* 1999; **400**: 256–261.
- 427 12. Sasaki A, Ashikari M, Ueguchi-Tanaka M, Itoh H, Nishimura A, Swapan D, et al. A mutant  
428 gibberellin-synthesis gene in rice. *Nature* 2002; **291**: 1–2.
- 429 13. Tully RE, Keister DL. Cloning and mutagenesis of a cytochrome P-450 locus from  
430 *Bradyrhizobium japonicum* that is expressed anaerobically and symbiotically. *Appl Environ*  
431 *Microbiol* 1993; **59**: 4136–4142.
- 432 14. Tully RE, Berkum P Van, Lovins KW, Keister DL. Identification and sequencing of a cytochrome  
433 P450 gene cluster from *Bradyrhizobium japonicum*. *Biochim Biophys Acta* 1998; **1398**: 243–255.
- 434 15. Keister DL, Tully RE, Berkum P Van. A cytochrome P450 gene cluster in the Rhizobiaceae. *J*  
435 *Gen Appl Microbiol* 1999; **45**: 301–303.
- 436 16. Morrone D, Chambers J, Lowry L, Kim G, Anterola A, Bender K, et al. Gibberellin biosynthesis  
437 in bacteria: Separate *ent*-copalyl diphosphate and *ent*-kaurene synthases in *Bradyrhizobium*  
438 *japonicum*. *FEBS Lett* 2009; **583**: 475–480.
- 439 17. Hershey DM, Lu X, Zi J, Peters RJ. Functional conservation of the capacity for *ent*-kaurene  
440 biosynthesis and an associated operon in certain rhizobia. *J Bacteriol* 2014; **196**: 100–106.

- 441 18. Méndez C, Baginsky C, Hedden P, Gong F, Carú M, Rojas MC. Gibberellin oxidase activities in  
442 *Bradyrhizobium japonicum* bacteroids. *Phytochemistry* 2014; **98**: 101–109.
- 443 19. Levy A, Salas Gonzalez I, Mittelviehhaus M, Clingenpeel S, Herrera Paredes S, Miao J, et al.  
444 Genomic features of bacterial adaptation to plants. *Nat Genet* 2018; **50**: 138–150.
- 445 20. Nagel R, Peters R. Investigating the phylogenetic range of gibberellin biosynthesis in bacteria.  
446 *Mol Plant-Microbe Interact* 2017; **30**: 343–349.
- 447 21. Nagel R, Bieber JE, Schmidt-Dannert MG, Nett RS, Peters RJ. A third class: Functional  
448 gibberellin biosynthetic operon in beta-proteobacteria. *Front Microbiol* 2018; **9**: 2916.
- 449 22. Nett RS, Contreras T, Peters RJ. Characterization of CYP115 as a gibberellin 3-oxidase indicates  
450 that certain rhizobia can produce bioactive gibberellin A<sub>4</sub>. *ACS Chem Biol* 2017; **12**: 912–917.
- 451 23. Berthelot K, Estevez Y, Deffieux A, Peruch F. Isopentenyl diphosphate isomerase: A checkpoint  
452 to isoprenoid biosynthesis. *Biochimie* 2012; **94**: 1621–1634.
- 453 24. Sullivan JT, Trzebiatowski JR, Brown SD, Elliot RM, Fleetwood DJ, Mccallum NG, et al.  
454 Comparative sequence analysis of the symbiosis island of *Mesorhizobium loti* strain R7A. *J*  
455 *Bacteriol* 2002; **184**: 3086–3095.
- 456 25. Ream DC, Bankapur AR, Friedberg I. An event-driven approach for studying gene block  
457 evolution in bacteria. *Bioinformatics* 2015; **31**: 2075–2083.
- 458 26. Freiberg C, Fellay R, Bairock A, Broughton WJ, Rosenthal A, Perret X. Molecular basis of  
459 symbiosis between *Rhizobium* and legumes. *Nature* 1997; **387**: 394–401.
- 460 27. González V, Bustos P, Ramírez-Romero M a, Medrano-Soto A, Salgado H, Hernández-González  
461 I, et al. The mosaic structure of the symbiotic plasmid of *Rhizobium etli* CFN42 and its relation to  
462 other symbiotic genome compartments. *Genome Biol* 2003; **4**: R36.

- 463 28. Lassalle F, Perian S, Bataillon T, Nesme X, Duret L, Daubin V. GC-content evolution in bacterial  
464 genomes: the biased gene conversion hypothesis expands. *PLoS Genet* 2015; **11**: e1004941.
- 465 29. Dobrindt U, Hochhut B, Hentschel U, Hacker J. Genomic islands in pathogenic and environmental  
466 microorganisms. *Nat Rev Microbiol* 2004; **2**: 414–424.
- 467 30. Göttfert M, Röthlisberger S, Kündig C, Beck C, Marty R, Hennecke H. Potential symbiosis-  
468 specific genes uncovered by sequencing a 410-kilobase DNA region of the *Bradyrhizobium*  
469 *japonicum* chromosome. *J Bacteriol* 2001; **183**: 1405–1412.
- 470 31. Kaneko T, Nakamura Y, Sato S, Minamisawa K, Uchiumi T, Sasamoto S, et al. Complete  
471 genomic sequence of nitrogen-fixing symbiotic bacterium *Bradyrhizobium japonicum* USDA110.  
472 *DNA Res* 2002; **9**: 189–197.
- 473 32. Uchiumi T, Ohwada T, Itakura M, Mitsui H, Nukui N, Dawadi P, et al. Expression islands  
474 clustered on the symbiosis island of the *Mesorhizobium loti* genome. *J Bacteriol* 2004; **186**: 2439–  
475 2448.
- 476 33. Nguyen HN, Jain A, Eulenstein O, Friedberg I. Tracing the ancestry of operons in bacteria.  
477 *Bioinformatics* 2019; **35**: 2998–3004.
- 478 34. Chernomor O, Minh BQ, Forest F, Klaere S, Ingram T, Henzinger M, et al. Split diversity in  
479 constrained conservation prioritization using integer linear programming. *Methods Ecol Evol*  
480 2015; **6**: 83–91.
- 481 35. Lemke C, Potter KC, Schulte S, Peters RJ. Conserved bases for the initial cyclase in gibberellin  
482 biosynthesis: from bacteria to plants. *Biochem J* 2019; Accepted; September 4, 2019 DOI:  
483 10.1042/BCJ201904.
- 484 36. Hedden P, Sponsel V. A century of gibberellin research. *J Plant Growth Regul* 2015; **34**: 740–760.
- 485 37. Navarro L, Bari R, Achard P, Lisón P, Nemri A, Harberd NP, et al. DELLAs control plant

- 486 immune responses by modulating the balance of jasmonic acid and salicylic acid signaling. *Curr*  
487 *Biol* 2008; **18**: 650–655.
- 488 38. Hou X, Lee LYC, Xia K, Yan Y, Yu H. DELLAs modulate jasmonate signaling via competitive  
489 binding to JAZs. *Dev Cell* 2010; **19**: 884–894.
- 490 39. Schwechheimer C. Gibberellin signaling in plants – the extended version. *Front Plant Sci* 2012; **2**:  
491 1–7.
- 492 40. Oldroyd GED, Murray JD, Poole PS, Downie JA. The rules of engagement in the legume-  
493 rhizobial symbiosis. *Annu Rev Genet* 2011; **45**: 119–144.
- 494 41. Hayashi S, Gresshoff PM, Ferguson BJ. Mechanistic action of gibberellins in legume nodulation. *J*  
495 *Integr Plant Biol* 2014; **56**: 971–8.
- 496 42. Ueguchi-Tanaka M, Ashikari M, Nakajima M, Itoh H, Katoh E, Kobayashi M, et al.  
497 *GIBBERELLIN INSENSITIVE DWARF1* encodes a soluble receptor for gibberellin. *Nature* 2005;  
498 **437**: 693–698.
- 499 43. McAdam EL, Reid JB, Foo E. Gibberellins promote nodule organogenesis but inhibit the infection  
500 stages of nodulation. *J Exp Bot* 2018; **69**: 2117–2130.
- 501 44. Noel KD, Sanchez A, Fernandez L, Leemans J, Cevallos MA. Rhizobium phaseoli symbiotic  
502 mutants with transposon Tn5 insertions. *J Bacteriol* 1984; **158**: 148–155.
- 503 45. Nagel R, Bernholz C, Vranov E, Kosuth J, Bergau N, Ludwig S, et al. *Arabidopsis thaliana*  
504 isoprenyl diphosphate synthases produce the C<sub>25</sub> intermediate geranylarnesyl diphosphate. *Plant J*  
505 2015; **84**: 847–859.
- 506 46. Seemann T. Prokka: Rapid prokaryotic genome annotation. *Bioinformatics* 2014; **30**: 2068–2069.  
507

## FIGURES

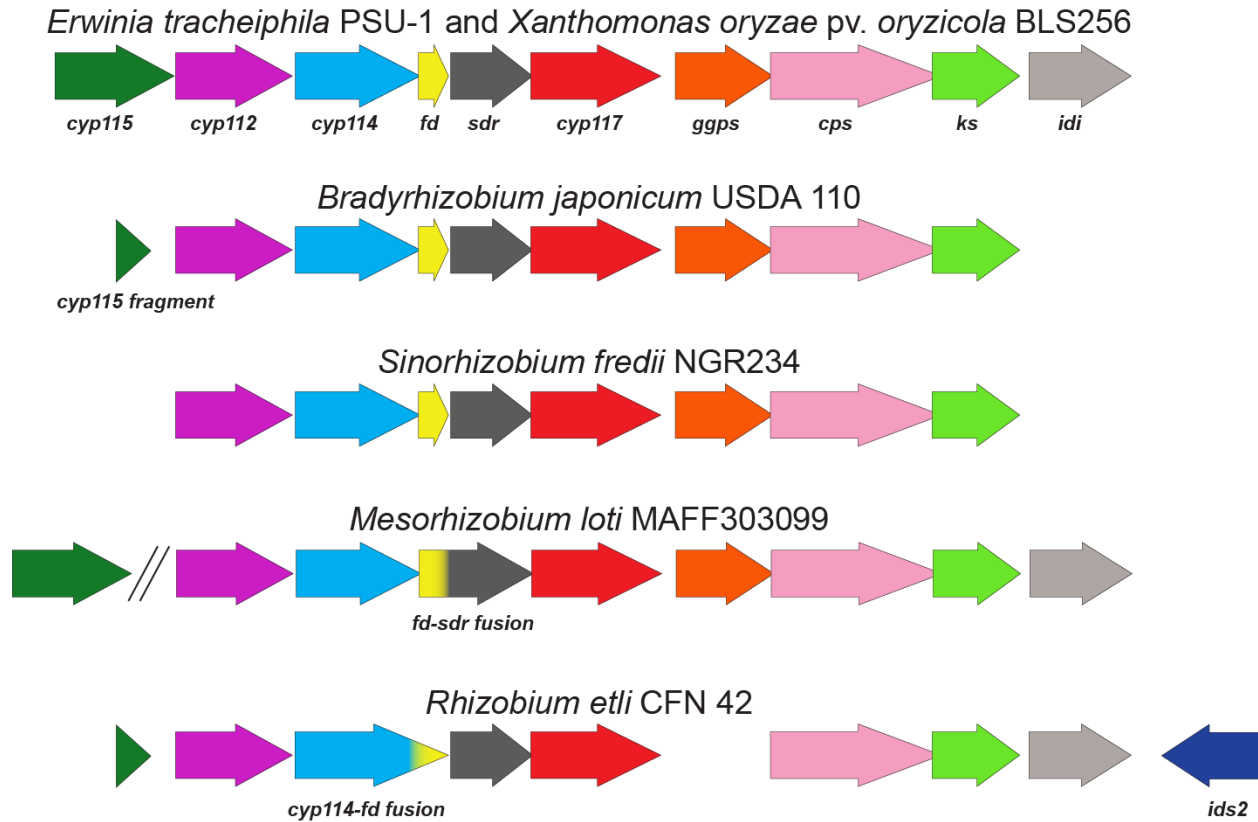


**Figure 1. Diversity among GA biosynthetic operons in divergent bacterial lineages.** The core operon genes are defined as *cyp112*, *cyp114*, *fd*, *sdr*, *cyp117*, *ggps*, *cps*, and *ks*, as these are almost always present within the GA operon. Other genes, including *cyp115*, *idi*, and *ids2*, exhibit a more limited distribution among GA operon-containing species. The tandem diagonal lines in the *Mesorhizobium loti* MAFF303099 operon indicates that *cyp115* is not located adjacent to the rest of the operon.







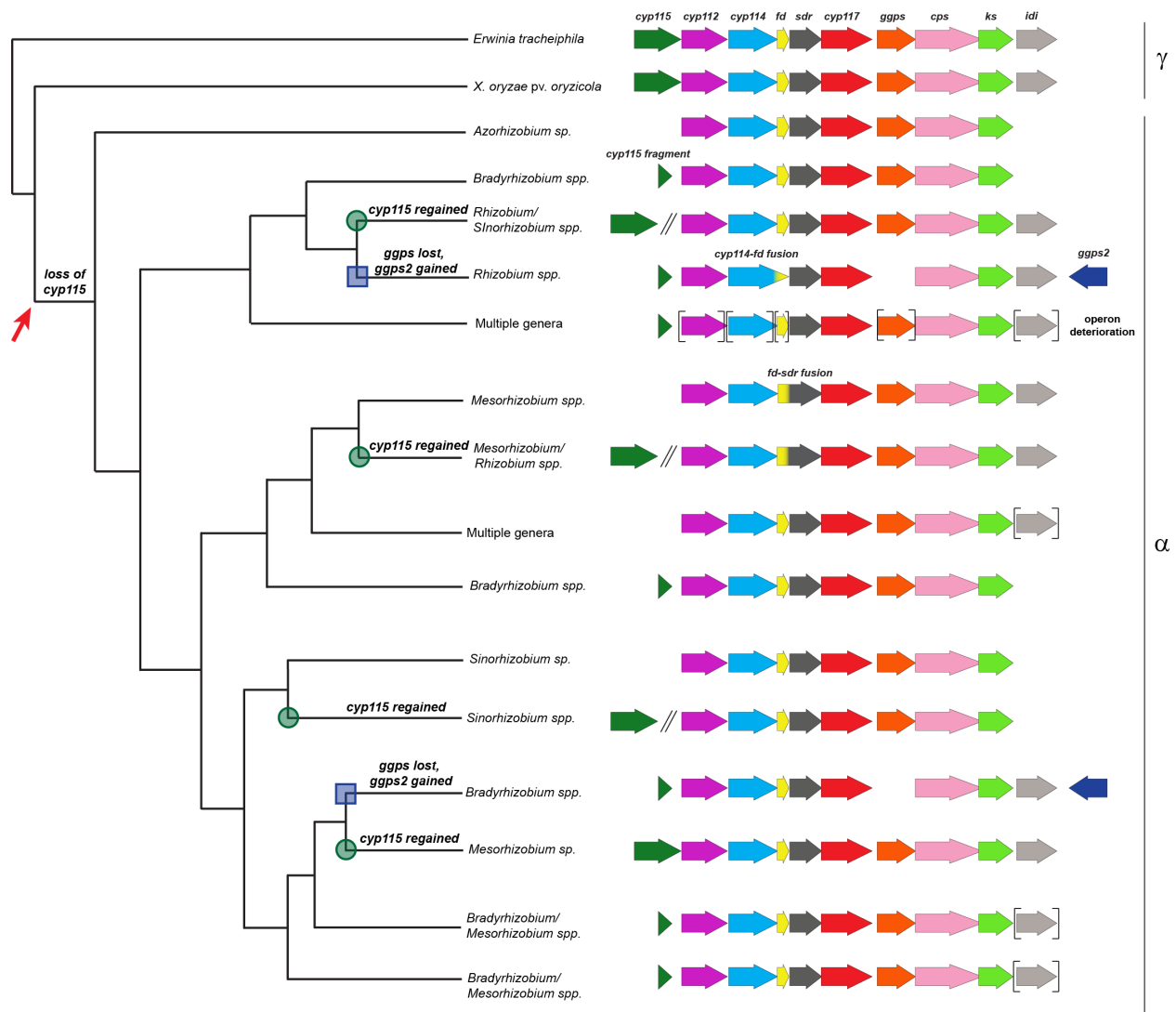


**Figure 4. Summary of ancestral reconstruction for the GA biosynthetic operon.** As a representation of GA operon evolution, the results from the full reconstruction generated using the concatenated operon (*FO*) are summarized here. Initial loss of the *cyp115* gene is indicated with a red arrow, while reacquisition of this gene is indicated with a green circle at the ancestral node. Loss of *ggps* and acquisition of *ggps2* is indicated by a blue box at the ancestral node. Brackets around a gene represent variable presence within that lineage. Double slanted lines indicate genes that are not located within the cluster (i.e. >500 bp away). The family of proteobacterial lineages is indicated to the right of the figure ( $\alpha$  and  $\gamma$  labels).